

Supplementary Online Content

Lee JS, Ruppin E. Multiomics prediction of response rates to therapies to inhibit programmed cell death 1 and programmed cell death 1 ligand 1. *JAMA Oncol.* Published online August 22, 2019. doi:10.1001/jamaoncol.2019.2311

eMethods. Tumor Neoantigen, Tumor Immune Microenvironment, Checkpoint Targets, and Statistics

eTable. ORR and Correlate Variables of Anti–PD-1/PD-L1 Therapy Across Cancer Types

eFigure 1. Systematic Evaluation of Correlates of Response to Anti–PD-1/PD-L1 Therapy Across Different Cancer Types

eFigure 2. Combination of MB, eCD8T and fPD1 to Predict Anti–PD-1/PD-L1 Response in Individual Cancer Types

eReferences.

This supplementary material has been provided by the authors to give readers additional information about their work.

eMethods. Tumor Neoantigen, Tumor Immune Microenvironment, Checkpoint Targets, and Statistics

We considered multiple variables that have been previously reported to be potentially associated with anti-PD1/PDL1 response, including tumor mutational burden (MB), intra-tumor heterogeneity (ITH)¹, estimated immune cell abundance of CD8+ T-cells, the cytolytic score², PDL1 protein expression, and the combined positive score (CPS)⁹. TCGA data was downloaded from UCSC Xena browser (<https://xenabrowser.net/>) for 9,935 samples in 34 cancer types, which preprocessed the original data from Genomic Data Commons (GDC) data portal. Twenty one out of the 34 cancer types whose objective response rate (ORR) data was available were used in subsequent analysis (N=7,187). The ORR data was obtained through personal communications with Yarchaoan *et al.*³ (as noted in Acknowledgement). The microsatellite instability data⁴ was used to classify MSI tumors in TCGA. The variables are classified in the following three types.

Tumor neoantigen

Tumor mutational burden was determined based on whole exome sequencing (WES) data of TCGA samples. The mutation call was performed using SomaticSniper⁵ and downloaded from UCSC Xena browser (https://gdc.xenahubs.net/download/GDC-PANCAN/Xena_Matrices/GDC-PANCAN.somaticsniper_snv.tsv.gz), and we counted the number of nonsynonymous single nucleotide variants (SNV) per given sample. ITH was calculated based on ABSOLUTE⁶ and the neoantigens were identified based on the neo-peptides predicted to bind to MHC-I, and downloaded from GDC panimmune data portal (<https://gdc.cancer.gov/about-data/publications/panimmune>)⁷. The hydrophobicity of the predicted neo-peptides was estimated via a computational model of peptide structure⁸, based on the notion that more hydrophobic peptides tend to be more immunogenic⁹.

Tumor immune microenvironment

We used the murine T-cell exhaustion signature¹⁰, where the gene list was obtained from Supp Table 6 of¹¹. The level of T-cell exhaustion was determined by the mean expression of the up-regulated genes subtracted by the mean expression of down-regulated genes. Immune cell abundance was determined by applying a computational deconvolution method¹². The FPKM-normalized mRNA expression data was downloaded from UCSC Xena browser (https://gdc.xenahubs.net/download/GDC-PANCAN/Xena_Matrices/GDC-PANCAN.htseq_fpkm.tsv.gz). The use of this approach is supported by the recent demonstration that the computational deconvolution methods can robustly estimate the immune cell infiltrates in the tumor with good accuracy especially for well-characterized cell types including CD8+ T-cells¹³. The cytolytic score is a measure of local immune cytolytic activity calculated by the geometric mean of gene expression of granzyme A (GZMA) and perforin (PRF1)². Anti-PD1 therapy specific IFN-γ signature and the extended immune signature were obtained from¹⁴. T-Cell receptor diversity was estimated from RNAseq using Shannon entropy, and downloaded from GDC panimmune data portal (<https://gdc.cancer.gov/about-data/publications/panimmune>)⁷.

Checkpoint targets

PDL1 protein expression was measured by reverse phase protein array (RPPA), and downloaded from UCSC Xena browser (<https://pancanatlas.xenahubs.net/download/TCGA-RPPA-pancan-clean.xena.gz>). CPS was calculated based on the RPPA PDL1 values and tumor

purity estimated by ABSOLUTE⁶. For fPD1, TPM-normalized gene expression data was obtained from Xena browser (https://toil.xenahubs.net/download/tcgab_RSEM_gene_tpm.gz), which preprocessed the original data from TCGA data portal, and the 80-percentile of PD1 expression across all samples were used as threshold.

The median values of each variable were calculated per each cancer type. The bi-variate and tri-variate regression analyses were performed with leave-one-out cross-validation. We performed an analogous analysis in a smaller subset of dataset (N=17) used in the study that identified fPD1 as a strong correlate to anti-PD1/PDL1 therapy¹⁵, where they reported fPD1 correlates with specific anti-PD1 (not anti-PDL1) ORR across cancer types.

For the analysis of Merkel cell carcinoma (MCC)¹⁴ and small cell lung cancer (SCLC)¹³, we calculated the MB, eCD8T, and fPD1 levels by counting nonsynonymous mutations, running CIBERSORT¹² on RNAseq data, and applying the 80-percentile of FPKM values from TCGA PD1 mRNA expression¹⁰, respectively. All data was available as Supplementary Material of both papers except the RNAseq data for MCC, which we obtained through personal communications with the authors (as noted in Acknowledgement). We used MB-univariate, MB-eCD8T bi-variate, and MB-eCD8T-fPD1 tri-variate models to predict ORR in these cancer types. In an independent cohort of melanoma patients¹⁶, we compared the patients' survival after anti-PD1/PDL1 treatment based on MB, eCD8T and their combined levels, where each of the variables were Z-score transformed. The survival of patients with high (top 50-percentile) vs low (bottom 50-percentile) levels were compared using logrank test.

Statistics

We performed a standard regression analysis with leave-one-out cross-validation in predicting ORR across cancer types using R package “caret.” The performance of the prediction was evaluated based on Spearman rank correlation (R) and unexplained variance (1-R²). For comparing goodness of fit between different models, log-likelihood ratio test was performed. The association between MB, eCD8T, their combination versus the patient survival after anti-PD1/PDL1 therapy in melanoma cohort was evaluated using logrank test. All P values are expressed to 2 digits to the right of the decimal point, or to 3 digits if <0.01.

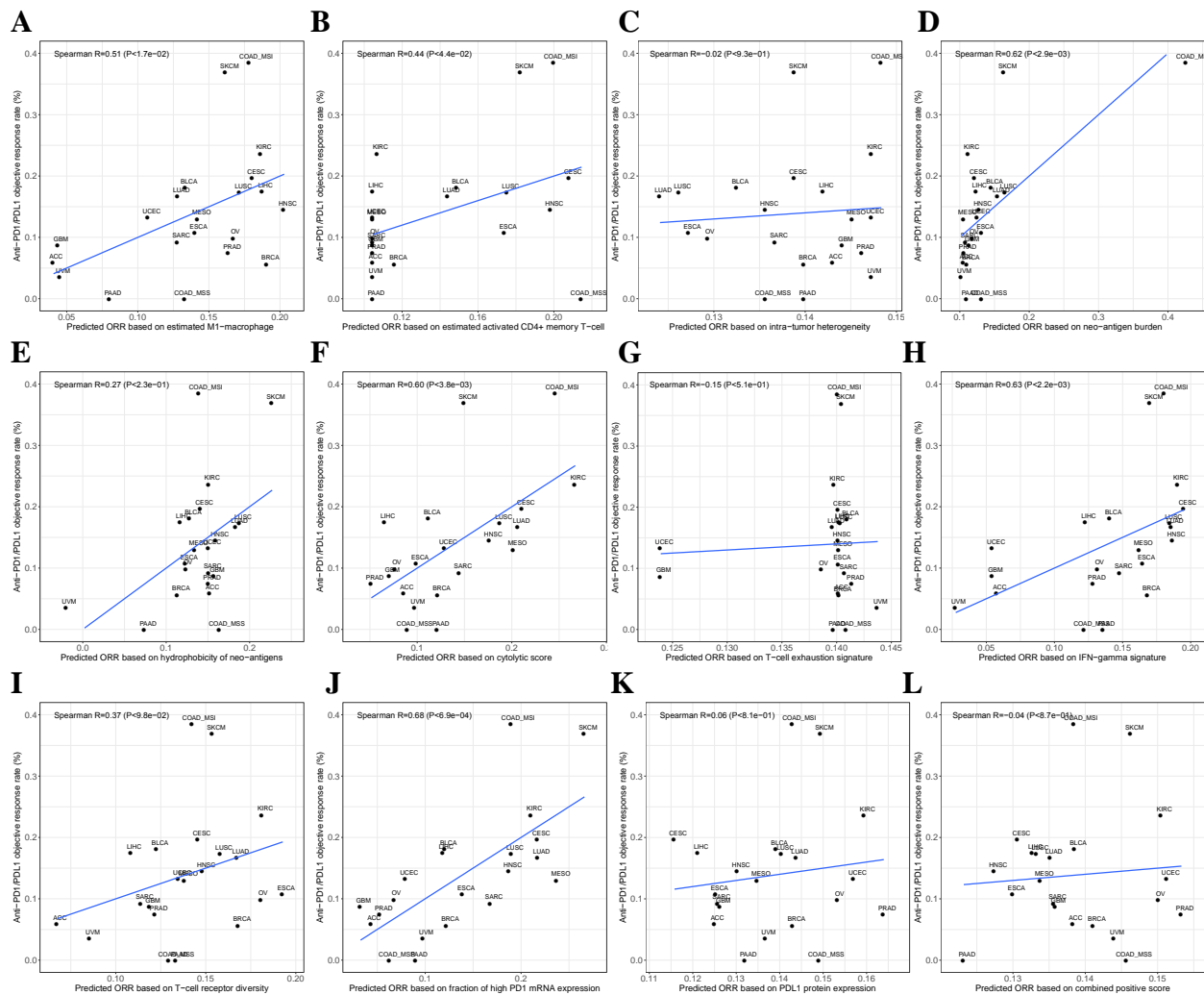
eTable. ORR and Correlate Variables of Anti–PD-1/PD-L1 Therapy Across Cancer Types

The table shows the ORR and the 36 variables considered in our analysis (in addition to tumor purity) across the 21 cancer types.

types	ACC	BRCA	CESC	COAD_MS1	COAD_MSS	UCEC	ESCA	GBM	HNSC	LIHC	SKCM
ORR	6.0E-02	5.7E-02	2.0E-01	3.9E-01	0.0E+00	1.3E-01	1.1E-01	8.7E-02	1.5E-01	1.8E-01	3.7E-01
Mutational Burden	1.7E+01	2.2E+01	5.9E+01	6.8E+02	6.7E+01	5.4E+01	6.9E+01	3.4E+01	5.3E+01	5.6E+01	2.1E+02
log10(MB)	1.2E+00	1.3E+00	1.8E+00	2.8E+00	1.8E+00	1.7E+00	1.8E+00	1.5E+00	1.7E+00	1.7E+00	2.3E+00
Cytolytic score	2.3E+00	2.9E+00	4.5E+00	5.1E+00	2.4E+00	3.0E+00	2.5E+00	2.0E+00	3.9E+00	1.9E+00	3.4E+00
T-cell exhaustion signature	-	-3.3E+02	-3.3E+02	-3.3E+02	-3.4E+02	0.0E+00	-3.3E+02	0.0E+00	-3.3E+02	-3.3E+02	-3.4E+02
IFNg signature	6.9E-01	2.4E+01	2.9E+01	2.6E+01	1.4E+01	0.0E+00	2.3E+01	0.0E+00	2.7E+01	1.4E+01	2.4E+01
Extended immune signature	0.0E+00	6.3E+01	7.7E+01	7.2E+01	4.1E+01	0.0E+00	6.0E+01	0.0E+00	7.2E+01	3.2E+01	6.7E+01
B-cell naïve	1.9E-02	5.6E-02	2.7E-02	4.6E-02	4.6E-02	5.7E-02	4.8E-02	2.2E-03	1.9E-02	4.0E-02	2.5E-02
B-cell memory	0.0E+00	0.0E+00	0.0E+00	0.0E+00	0.0E+00	0.0E+00	0.0E+00	0.0E+00	0.0E+00	0.0E+00	0.0E+00
Plasma cells	8.9E-04	1.1E-02	1.4E-02	4.1E-03	6.6E-03	1.2E-02	7.5E-03	5.7E-05	1.5E-02	4.1E-03	7.5E-03
CD8+ T-cells	6.2E-02	8.2E-02	1.5E-01	1.3E-01	7.7E-02	1.1E-01	5.6E-02	7.7E-03	8.0E-02	9.9E-02	1.5E-01
CD4+ naïve T-cells	0.0E+00	0.0E+00	0.0E+00	0.0E+00	0.0E+00	0.0E+00	0.0E+00	0.0E+00	0.0E+00	0.0E+00	0.0E+00
CD4+ resting T-cells	2.0E-01	1.5E-01	8.2E-02	1.4E-01	1.7E-01	1.5E-01	2.1E-01	1.1E-01	1.1E-01	1.6E-01	5.8E-02
CD4+ active T-cells	0.0E+00	5.7E-03	5.1E-02	4.7E-02	5.4E-02	0.0E+00	3.4E-02	0.0E+00	4.6E-02	0.0E+00	3.8E-02
CD4+ helper T-cells	0.0E+00	3.6E-02	4.7E-02	1.9E-02	1.1E-02	3.8E-02	1.6E-02	7.5E-03	2.6E-02	1.4E-03	4.3E-02
T-reg	0.0E+00	1.7E-02	2.5E-02	1.3E-02	1.0E-02	3.6E-02	1.2E-02	6.9E-03	6.3E-03	2.9E-02	2.6E-02
T-cell gamma delta	0.0E+00	0.0E+00	0.0E+00	0.0E+00	0.0E+00	0.0E+00	0.0E+00	0.0E+00	0.0E+00	0.0E+00	0.0E+00
Resting NK cells	0.0E+00	0.0E+00	0.0E+00	2.2E-02	3.9E-03	0.0E+00	3.8E-03	1.1E-02	1.5E-02	0.0E+00	0.0E+00
Active NK cells	3.3E-02	5.7E-03	3.3E-02	1.0E-02	0.0E+00	4.6E-02	7.7E-04	1.2E-02	2.3E-04	5.1E-02	1.5E-02
Monocytes	6.3E-02	0.0E+00	0.0E+00	0.0E+00	0.0E+00	1.1E-03	1.1E-01	0.0E+00	1.7E-02	7.4E-03	
M0 macrophage	1.3E-02	1.7E-01	1.0E-01	2.0E-01	2.1E-01	1.7E-01	1.3E-01	7.9E-02	2.0E-01	9.4E-02	1.5E-01
M1 macrophage	1.8E-02	8.0E-02	7.6E-02	7.5E-02	5.6E-02	4.5E-02	5.9E-02	1.9E-02	8.5E-02	7.9E-02	6.8E-02
M2 macrophage	2.2E-01	1.4E-01	7.2E-02	1.1E-01	1.1E-01	7.8E-02	7.7E-02	3.6E-01	9.0E-02	1.6E-01	1.3E-01
Resting dendritic cells	0.0E+00	6.9E-03	1.6E-02	4.4E-03	8.1E-03	0.0E+00	4.4E-03	0.0E+00	2.4E-02	1.5E-02	4.6E-03
Active dendritic cells	4.3E-02	0.0E+00	2.3E-02	0.0E+00	0.0E+00	2.7E-02	0.0E+00	1.8E-02	0.0E+00	0.0E+00	0.0E+00
Resting mast cells	5.7E-02	6.4E-02	3.6E-02	0.0E+00	0.0E+00	2.7E-02	4.5E-03	6.6E-03	1.9E-02	6.0E-02	3.3E-02
Active mast cells	0.0E+00	0.0E+00	0.0E+00	7.4E-03	1.2E-02	0.0E+00	6.5E-04	0.0E+00	0.0E+00	0.0E+00	0.0E+00
Eosinophils	0.0E+00	0.0E+00	0.0E+00	0.0E+00	0.0E+00	0.0E+00	0.0E+00	0.0E+00	0.0E+00	0.0E+00	0.0E+00
Neutrophils	0.0E+00	0.0E+00	0.0E+00	1.1E-04	0.0E+00	0.0E+00	0.0E+00	1.1E-02	2.9E-03	0.0E+00	0.0E+00
ITH	6.0E-02	9.0E-02	1.0E-01	1.0E-02	1.3E-01	2.0E-02	2.1E-01	5.0E-02	1.3E-01	7.0E-02	1.0E-01
PDL1 protein expression	4.1E-01	9.5E-02	5.8E-01	9.7E-02	-9.7E-03	-1.5E-01	4.1E-01	3.9E-01	3.2E-01	4.8E-01	-1.7E-02
PDL1 gene expression	-	1.5E+00	2.3E+00	1.9E+00	1.0E+00	1.2E+00	7.5E+01	1.9E+01	1.7E+00	6.3E+01	1.4E+00
PDI gene expression	-	-6.9E-01	3.8E-01	2.3E-01	-7.1E-01	-2.1E-01	-1.7E-01	-1.8E+00	7.2E+02	-1.6E+00	5.9E+01
IPD1	2.2E-02	1.5E-01	3.1E-01	2.7E-01	5.4E-02	8.1E-02	1.8E-01	2.6E-03	2.6E-01	1.5E-01	3.9E-01
Neoantigen burden	3.5E+01	5.7E+01	1.1E+02	1.5E+03	1.5E+02	1.2E+02	1.5E+02	7.1E+01	1.4E+02	1.2E+02	3.0E+02
Hydrophobicity of neoantigen	1.4E+00	1.4E+00	1.4E+00	1.4E+00	1.4E+00	1.4E+00	1.4E+00	1.4E+00	1.4E+00	1.4E+00	1.4E+00
CPS	8.8E-01	7.5E-01	1.2E+00	8.7E-01	5.4E-01	2.8E-01	1.3E+00	9.9E-01	1.4E+00	1.1E+00	5.1E-01
TCR diversity	6.9E-01	2.9E+00	2.4E+00	2.4E+00	2.1E+00	2.2E+00	3.5E+00	1.8E+00	2.5E+00	1.6E+00	2.6E+00
Tumor purity	8.4E-01	6.0E-01	6.7E-01	5.6E-01	6.5E-01	7.6E-01	6.1E-01	7.8E-01	4.9E-01	7.2E-01	7.0E-01
types	MESO	UVM	LUAD	LUSC	OV	PAAD	PRAD	KIRC	SARC	BLCA	
ORR	1.3E-01	3.6E-02	1.7E-01	1.7E-01	9.9E-02	0.0E+00	7.5E-02	2.4E-01	9.3E-02	1.8E-01	
Mutational Burden	1.7E+01	9.0E+00	9.2E+01	1.4E+02	3.8E+01	1.6E+01	1.3E+01	2.6E+01	2.6E+01	9.5E+01	
log10(MB)	1.2E+00	9.5E+01	2.0E+00	2.1E+00	1.6E+00	1.2E+00	1.1E+00	1.4E+00	1.4E+00	2.0E+00	
Cytolytic score	4.3E+00	2.5E+00	4.4E+00	4.0E+00	2.1E+00	2.9E+00	1.7E+00	5.4E+00	3.3E+00	2.7E+00	
T-cell exhaustion signature	-	-4.0E+02	-3.2E+02	-3.3E+02	-3.0E+02	-3.2E+02	-3.6E+02	-3.2E+02	-3.4E+02	-3.5E+02	
IFNg signature	2.2E+01	-5.6E+00	2.7E+01	2.7E+01	1.6E+01	1.7E+01	1.5E+01	2.8E+01	1.9E+01	1.8E+01	
Extended immune signature	6.4E+01	-1.7E+01	7.8E+01	7.4E+01	3.6E+01	5.3E+01	3.9E+01	7.9E+01	4.8E+01	4.9E+01	
B-cell naïve	3.4E-02	2.9E-04	8.1E-02	7.7E-02	2.9E-02	4.2E-02	6.3E-02	3.0E-02	7.5E-03	1.9E-02	
B-cell memory	0.0E+00	0.0E+00	0.0E+00	0.0E+00	0.0E+00	0.0E+00	0.0E+00	0.0E+00	0.0E+00	0.0E+00	
Plasma cells	5.0E-03	2.4E-02	5.7E-02	5.8E-02	1.1E-03	1.7E-03	2.1E-02	6.2E-03	8.1E-04	1.1E-02	
CD8+ T-cells	9.6E-02	8.2E-02	8.3E-02	9.1E-02	5.6E-02	6.5E-02	1.1E-01	1.6E-01	1.6E-01	6.5E-02	1.1E-01
CD4+ naïve T-cells	0.0E+00	0.0E+00	0.0E+00	0.0E+00	0.0E+00	0.0E+00	0.0E+00	0.0E+00	0.0E+00	0.0E+00	0.0E+00
CD4+ resting T-cells	1.5E-01	1.1E-01	1.3E-01	1.1E-01	1.9E-01	1.7E-01	2.4E-01	1.8E-01	1.3E-01	9.1E-02	
CD4+ active T-cells	0.0E+00	0.0E+00	1.9E-02	3.4E-02	0.0E+00	0.0E+00	0.0E+00	1.2E-03	0.0E+00	2.2E-02	
CD4+ helper T-cells	2.3E-02	2.4E-03	2.1E-02	2.4E-02	2.4E-02	0.0E+00	2.7E-02	2.1E-03	9.8E-03	3.2E-02	
T-reg	1.5E-02	1.5E-02	1.6E-02	3.1E-03	2.5E-02	2.6E-02	0.0E+00	1.1E-02	1.4E-02	1.1E-02	
T-cell gamma delta	0.0E+00	0.0E+00	0.0E+00	0.0E+00	0.0E+00	0.0E+00	0.0E+00	0.0E+00	0.0E+00	0.0E+00	
Resting NK cells	0.0E+00	0.0E+00	0.0E+00	5.0E-03	0.0E+00	0.0E+00	0.0E+00	0.0E+00	0.0E+00	0.0E+00	
Active NK cells	5.8E-02	4.5E-02	1.4E-02	2.2E-03	4.1E-02	1.6E-02	3.5E-02	2.8E-02	2.7E-02	1.7E-02	
Monocytes	8.5E-02	2.7E-02	6.3E-03	0.0E+00	1.9E-02	5.2E-03	1.1E-02	4.0E-02	2.4E-02	6.5E-03	
M0 macrophage	4.4E-02	1.1E-01	1.2E-01	1.8E-01	1.5E-01	1.9E-01	7.2E-02	9.6E-03	5.0E-02	9.9E-02	
M1 macrophage	6.0E-02	2.0E-02	5.4E-02	7.2E-02	7.0E-02	3.4E-02	6.9E-02	7.8E-02	5.4E-02	5.6E-02	
M2 macrophage	1.9E-01	2.9E-01	1.2E-01	1.1E-01	1.5E-01	1.5E-01	9.5E-02	1.9E-01	2.8E-01	1.1E-01	

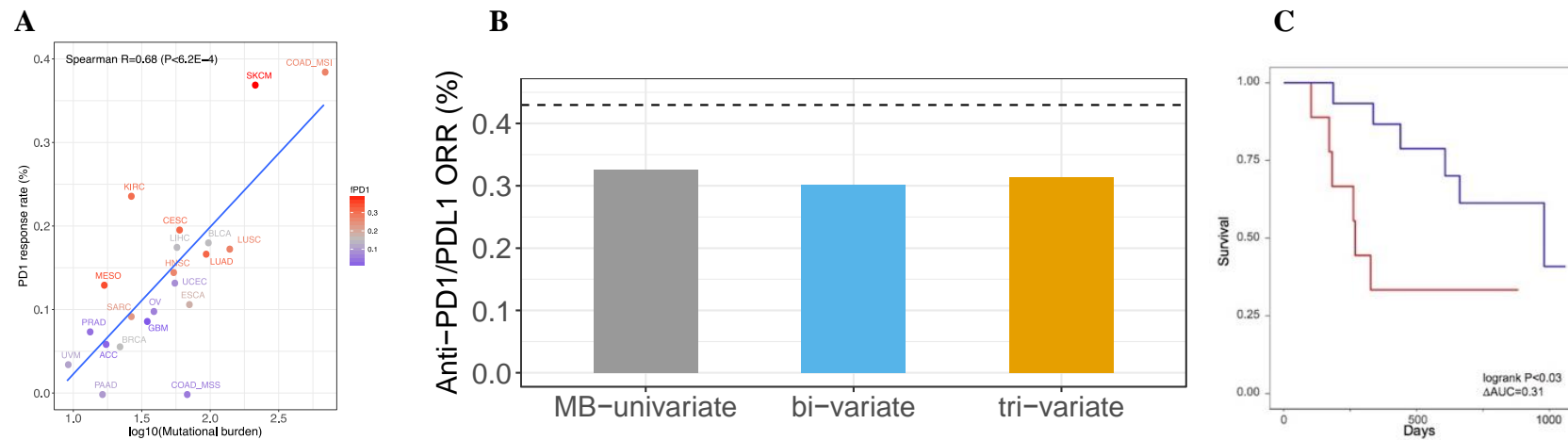
Resting dendritic cells	0.0E+00	6.5E-04	1.8E-02	1.0E-02	0.0E+00	2.7E-02	1.6E-02	2.4E-03	0.0E+00	1.2E-02	
Active dendritic cells	0.0E+00	0.0E+00	6.8E-03	0.0E+00	0.0E+00	5.2E-04	0.0E+00	0.0E+00	0.0E+00	2.6E-02	
Resting mast cells	3.2E-02	1.1E-01	5.0E-02	3.5E-02	7.5E-03	6.1E-02	1.2E-01	4.6E-02	6.0E-02	4.3E-02	
Active mast cells	0.0E+00	0.0E+00	0.0E+00	0.0E+00	0.0E+00	0.0E+00	0.0E+00	0.0E+00	0.0E+00	0.0E+00	
Eosinophils	0.0E+00	0.0E+00	0.0E+00	0.0E+00	0.0E+00	0.0E+00	0.0E+00	0.0E+00	0.0E+00	0.0E+00	
Neutrophils	0.0E+00	0.0E+00	4.0E-03	3.3E-03	0.0E+00	6.2E-04	0.0E+00	1.1E-03	0.0E+00	0.0E+00	
ITH	4.0E-02	2.0E-02	2.4E-01	2.2E-01	1.9E-01	9.0E-02	3.0E-02	2.0E-02	1.2E-01	1.6E-01	
PDL1 protein expression	2.4E-01	2.1E-01	8.2E-02	1.4E-01	-8.5E-02	2.9E-01	-2.7E-01	-1.9E-01	4.0E-01	1.6E-01	
PDL1 gene expression	2.1E+00	-1.6E+00	2.3E+00	1.9E+00	9.9E-02	1.4E+00	4.1E-01	2.8E+00	9.1E-01	1.0E+00	
PDI gene expression	8.1E-01	-3.5E+00	6.1E-01	3.6E-01	-8.3E-01	-7.3E-01	-1.2E+00	2.2E-01	-7.5E-01	-9.1E-01	
PD1	3.5E-01	1.1E-01	3.1E-01	2.7E-01	6.2E-02	9.9E-02	3.7E-02	3.0E-01	2.3E-01	1.5E-01	
Neoantigen burden	3.6E+01	2.0E+01	2.6E+02	3.0E+02	9.1E+01	5.4E+01	3.7E+01	6.6E+01	4.9E+01	2.1E+02	
Hydrophobicity of neoantigen	1.4E+00	1.3E+00	1.4E+00	1.4E+00	1.4E+00	1.4E+00	1.4E+00	1.4E+00	1.4E+00	1.4E+00	
CPS	1.1E+00	6.2E-01	1.0E+00	1.1E+00	3.4E-01	1.6E+00	2.0E-01	3.2E-01	1.0E+00	8.6E-01	
TCR diversity	2.3E+00	1.1E+00	2.9E+00	2.7E+00	3.2E+00	2.2E+00	1.9E+00	3.2E+00	1.7E+00	1.9E+00	
Tumor purity	6.4E-01	9.5E-01	4.5E-01	5.0E-01	8.0E-01	3.9E-01	6.1E-01	5.6E-01	7.8E-01	6.1E-01	

eFigure 1. Systematic Evaluation of Correlates of Response to Anti–PD-1/PD-L1 Therapy Across Different Cancer Types



Correlation of (A) estimated M1-macrophage abundance, (B) estimated active CD4+ memory T-cell abundance, (C) intratumor heterogeneity, (D) neoantigen burden, (E) hydrophobicity of neoantigens, (F) cytolytic score, (G) T-cell exhaustion, (H) IFN- γ signature (I) TCR diversity, (J) fraction of high PD1 mRNA expression, (K) PDL1 protein expression, and (L) combined positive score (right, X-axis) with the objective response rate to anti-PD1/PDL1 therapy (Y-axis) across cancer types.

eFigure 2. Combination of MB, eCD8T and fPD1 to Predict Anti–PD-1/PD-L1 Response in Individual Cancer Types



(A) Correlation of $\log_{10}(\text{MB})$ (X-axis) with the response rate to PD1/PDL1 therapy (Y-axis) across cancer types. The fPD1 of each cancer type is color coded where red color denotes high abundance and blue color denotes low abundance. (B) The predicted ORR to anti-PD1/PDL1 therapy in polyomavirus-negative MCC using a univariate MB model (grey), the MB-eCD8T bivariate model (blue) and the MB-eCD8T-fPD1 tri-variate model (yellow). The actual ORR is depicted with the dotted line. (C) The patients with higher predicted response rate (blue) show better prognosis after PD1/PDL1 treatment in melanoma than the patients with lower predicted response rate (red), where the patients were partitioned above and below the median predicted response rate.

eReferences

- 1 Raynaud, F., Mina, M., Tavernari, D. & Ciriello, G. Pan-cancer inference of intra-tumor heterogeneity reveals associations with different forms of genomic instability. *PLoS Genet* **14**, e1007669, doi:10.1371/journal.pgen.1007669 (2018).
- 2 Rooney, M. S., Shukla, S. A., Wu, C. J., Getz, G. & Hacohen, N. Molecular and genetic properties of tumors associated with local immune cytolytic activity. *Cell* **160**, 48-61, doi:10.1016/j.cell.2014.12.033 (2015).
- 3 Yarchoan, M., Hopkins, A. & Jaffee, E. M. Tumor Mutational Burden and Response Rate to PD-1 Inhibition. *N Engl J Med* **377**, 2500-2501, doi:10.1056/NEJMc1713444 (2017).
- 4 Cortes-Ciriano, I., Lee, S., Park, W. Y., Kim, T. M. & Park, P. J. A molecular portrait of microsatellite instability across multiple cancers. *Nat Commun* **8**, 15180, doi:10.1038/ncomms15180 (2017).
- 5 Larson, D. E. *et al.* SomaticSniper: identification of somatic point mutations in whole genome sequencing data. *Bioinformatics* **28**, 311-317, doi:10.1093/bioinformatics/btr665 (2012).
- 6 Carter, S. L. *et al.* Absolute quantification of somatic DNA alterations in human cancer. *Nat Biotechnol* **30**, 413-421, doi:10.1038/nbt.2203 (2012).
- 7 Thorsson, V. *et al.* The Immune Landscape of Cancer. *Immunity* **48**, 812-830 e814, doi:10.1016/j.immuni.2018.03.023 (2018).
- 8 Goldsack, D. E. & Chalifoux, R. C. Contribution of the free energy of mixing of hydrophobic side chains to the stability of the tertiary structure of proteins. *J Theor Biol* **39**, 645-651 (1973).
- 9 Chowell, D. *et al.* TCR contact residue hydrophobicity is a hallmark of immunogenic CD8+ T cell epitopes. *Proc Natl Acad Sci U S A* **112**, E1754-1762, doi:10.1073/pnas.1500973112 (2015).
- 10 Wherry, E. J. *et al.* Molecular signature of CD8+ T cell exhaustion during chronic viral infection. *Immunity* **27**, 670-684, doi:10.1016/j.immuni.2007.09.006 (2007).
- 11 McKinney, E. F., Lee, J. C., Jayne, D. R., Lyons, P. A. & Smith, K. G. T-cell exhaustion, co-stimulation and clinical outcome in autoimmunity and infection. *Nature* **523**, 612-616, doi:10.1038/nature14468 (2015).
- 12 Newman, A. M. *et al.* Robust enumeration of cell subsets from tissue expression profiles. *Nat Methods* **12**, 453-457, doi:10.1038/nmeth.3337 (2015).
- 13 Sturm, G. *et al.* Comprehensive evaluation of cell-type quantification methods for immuno-oncology. *biorxiv* (2018).
- 14 Ayers, M. *et al.* IFN-gamma-related mRNA profile predicts clinical response to PD-1 blockade. *J Clin Invest* **127**, 2930-2940, doi:10.1172/JCI91190 (2017).
- 15 Pare, L. *et al.* Association between PD1 mRNA and response to anti-PD1 monotherapy across multiple cancer types. *Ann Oncol* **29**, 2121-2128, doi:10.1093/annonc/mdy335 (2018).
- 16 Hugo, W. *et al.* Genomic and Transcriptomic Features of Response to Anti-PD-1 Therapy in Metastatic Melanoma. *Cell* **165**, 35-44, doi:10.1016/j.cell.2016.02.065 (2016).